CrossMark

ORIGINAL PAPER

Process engineering studies on gold nanoparticle formation via dynamic spectroscopic approach

Anirban Chakraborty[1] · Sampa Chakraborty[2] · Basab Chaudhuri[3] ·
Sekhar Bhattacharjee[4]

Abstract The present paper reports a systematic study on kinetics of formation of metal nanoparticles from their precursors. Synthesis of gold nanoparticles (AuNPs) from chloroauric acid by the Turkevich method was selected as a model reaction where trisodium citrate acted as a reducing agent and stabilizer. Time-variant concentration of chloroauric acid was measured directly by monitoring UV spectroscopic absorbance at 212.5 nm and cross-checked by iodometric titration method. The reaction was suitably modeled by pseudo-first-order kinetics, and rate constant value [$k = (7.93 \pm 0.67) \times 10^{-3}$ s^{-1}] at a fixed baseline condition was reported. Morphological studies on particle growth mechanism were done by atomic force microscopy (AFM). Effects of process variables—initial molar ratio of reactants (0.37–5.21), temperature (333–373 K), and pH (3.6–6.5)—on kinetic parameters were investigated. Fastest reaction rate and spherical particle symmetry were observed at an optimal reductant to precursor ratio of 1.33. From an Arrhenius plot of rate constant data, preexponential factor ($A = 8.013 \pm 0.896$ mM s^{-1}) and activation energy ($E_a = 21.69 \pm 2.3$ kJ mol^{-1}) were calculated. A global kinetic equation for AuNP synthesis has been determined. Process conditions for synthesis of mature AuNPs with optical and morphological characteristics suitable for biomedical applications were identified.

Keywords Gold nanoparticles · Surface morphology · Reduction kinetics

Nomenclature

C_A Concentration of chloroauric acid at time t (mM)
C_{A0} Initial concentration of chloroauric acid (mM)
C_B Concentration of trisodium citrate at time t (mM)
C_{B0} Initial concentration of trisodium citrate (mM)
k_0 Reaction rate constant defined by Eq. 2
k Pseudo-first-order reaction rate constant (s^{-1}) defined by Eq. 3
M Initial molar ratio (C_{B0}/C_{A0})
R Universal gas constant (J mol^{-1} K^{-1})
t Time (s)
T Temperature (K)

Introduction

Gold nanoparticles possess distinct optical [1], spectroscopic [2], and catalytic properties [3, 4]. Extensive research reports were published in the last decade on preparation, characterization, and application of gold nanoparticles (AuNPs) for bioimaging, protein conjugation, and drug delivery [5–8]. AuNPs are generally produced by the standard Turkevich method [9]—reduction of chloroauric acid (HAuCl$_4$) with trisodium citrate. This method was introduced by Turkevich in 1951 [9] and later refined by Frens in the 1970s [10]. Daniel and Astruc [7] published an excellent review on AuNPs and their various applications. Sivaraman et al. [11, 12] have provided conclusive

✉ Sekhar Bhattacharjee
  sekhar.bhatta@petronas.com.my

1 Presidency University, 86/1 College Street, Kolkata 700 073, India

2 Department of Chemical Engineering, University of Calcutta, 92, A.P.C. Road, Kolkata 700 009, India

3 West Bengal State University, North 24 Paraganas, Barasat 700126, India

4 Department of Chemical Engineering, Universiti Teknologi PETRONAS, 32610 Bandar Seri Iskandar, Malaysia

experimental evidences demonstrating that the sequence of addition of the gold precursor and reducing agent has a profound influence on size and stability of AuNPs.

Proper understanding of reaction kinetics and growth mechanism is important for controlling size, shape, and stability of metal nanoparticles. Extensive research data were published in the last decade on preparative methods, reaction mechanisms, and morphology of nanoparticles during their formation and maturing stages [13, 14]. However, till date, very limited information is available on kinetic parameters of AuNP synthesis reactions [15, 16]. Pacławski et al. [15] used the modified Finke-Watzky model [17] to derive rate parameters for AuNP formation using hydrazine sulfate as reductant. Patakfalvi et al. [18] used the same model to evaluate rate constants for silver nanoparticle synthesis reaction. The prime objective of our research endeavor was to make an attempt to bridge the information gap—i.e., to collect experimental data on precursor time–concentration profiles under various process conditions and correlate experimental data with a standard kinetic model. The classical Turkevich method was selected as a model reaction, and experimental data on reaction rate, AuNP diameter, and surface morphology were collected during birth, evolution, and maturing phases of AuNP in the reaction medium. Although the experimental protocol reported here was developed and demonstrated for AuNP synthesis, this methodology may be applied to study reaction kinetics and time-dependent morphology during formation of other metal nanoparticles.

Experimental section

Materials

Crystalline chloroauric acid ($HAuCl_4 \cdot 3H_2O$) manufactured by s.d. fine-Chem Private Limited (minimum assay as Au 49.0 %), trisodium citrate dihydrate ($C_6H_5Na_3O_7 \cdot 2H_2O$) manufactured by Merck Specialties Private Limited, and triple-distilled water obtained from our laboratory distillation plant were used.

Instruments

UV-Vis spectroscopy was performed with Hitachi U-4100 spectrophotometer with a resolution of 1 nm between 450 and 650 nm at room temperature. The spectrophotometer was used to measure directly the concentration of chloroauric acid and surface plasmon resonance (SPR) of the reaction medium [19]. DLS instrument (Malvern, ZetasizerNano ZS) was used to analyze hydrodynamic mean diameter and size distribution of AuNPs in the

samples collected. Tapping mode AFM (Veeco, Multimode, NanoscopeIIIa) measurement was performed under ambient conditions for all samples collected during reaction. One drop of collected samples was taken on a freshly cleaved mica sheet and dried, and RTESP (Si nitride) tip of resonant frequency 312.14 kHz was used for AFM imaging. Sizes and shapes of synthesized AuNPs were analyzed using a FEI Tecnai 12 BioTwin Transmission Electron Microscope (TEM) operating at 100 kV. Samples were prepared for electron microscopy by evaporating 2 μl of nanoparticle solution (at 25 °C) on Formvar-coated copper grids.

Preparation of AuNPs

AuNPs were prepared by the well-known Turkevich method [9, 16]. Fifty milliliters of 0.254 mM solution of chloroauric acid (pH 3.2) was heated and stirred continuously on a hot plate magnetic stirrer (MINATO-MT 400), and 0.5 ml 34 mM sodium citrate (pH 8.44) solution was added to the boiling chloroauric acid solution. On addition of citrate color of the solution gradually changed from colorless to gray to black to violet to purple to maroon red and eventually to wine red in about 200–250 s (Figs. 1 and 2). During reaction, pH of the reaction medium remained nearly constant at 3.6. Aliquot samples (2 ml) of the reaction medium (from colorless to wine red) were collected at definite time intervals using a micropipette and kept under freezing condition (275 ± 2 K) for further analysis. Ojea-Jimenez [20] has used similar techniques for sample preservation (+4 °C) and analysis. Time–concentration profiles of chloroauric acid were determined using iodometric and spectroscopic methods [19].

Process conditions play a vital role in AuNP synthesis mechanism and determination of their size, shape, and dispersity [13, 21–23]. To study the effects of reaction conditions on AuNP formation kinetics, experiments were first carried out at a fixed baseline condition: $M = 1.33 \pm 0.053$ (50 ml 0.254 mM chloroauric acid and 0.5 ml of 0.34 mM sodium citrate solutions) and $T = 373 \pm 1$ K. AuNP synthesis experiments were also carried out by changing molar ratio of the reactants ($M = 0.37$–5.21), temperature (333–373 K), and pH (3.6–6.5) of the reaction medium. Stirrer speed in all experiments was always maintained at 600 rpm.

Results and discussion

AuNP synthesis by the Turkevich method has been studied extensively [7, 21, 22] and a host of reaction mechanisms and reaction intermediates were proposed by several researchers [22, 24]. Although time-resolved optical characterizations of AuNPs were studied by several investigators [23, 25], interpretation of spectroscopy data

Fig. 1 UV-Vis spectra and colors of aliquot samples collected during baseline reaction ($M = 1.33$, $T = 373$ K)
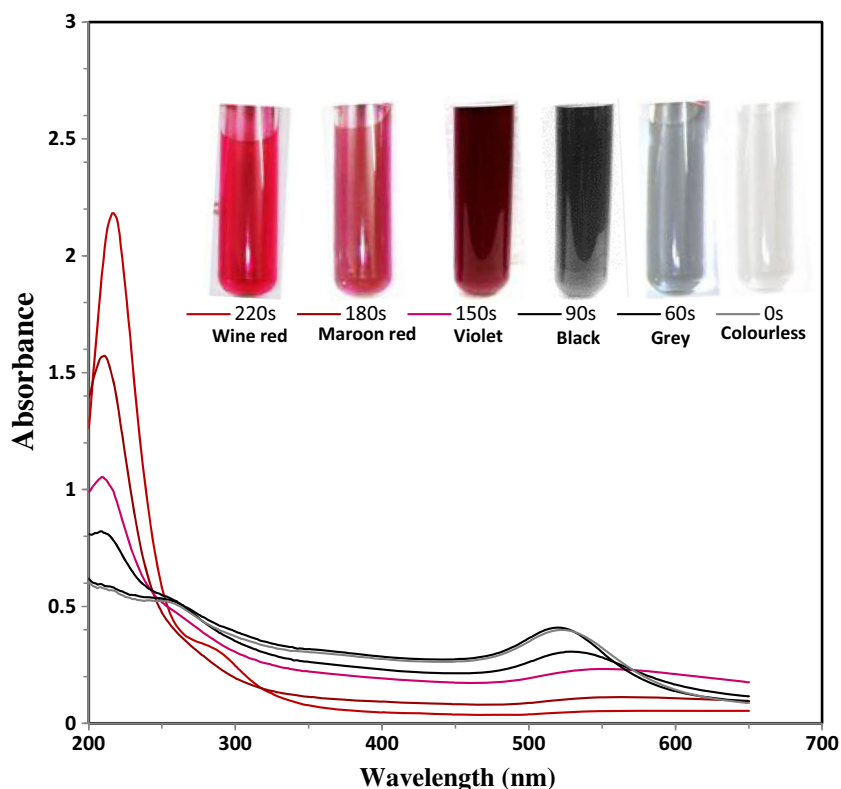

and growth mechanism of AuNP remain controversial and are yet to be ascertained conclusively. Kumer et al. [22] suggested that the crucial step of AuNP formation is

oxidation of citrate to dicarboxyacetone followed by reduction of auric to aurous ion and disproportionation of aurous ions to gold atoms. Overall stoichiometry of

Fig. 2 SPR wavelength and absorbance vs. time profiles under baseline reaction condition ($M = 1.33$, $T = 373$ K)
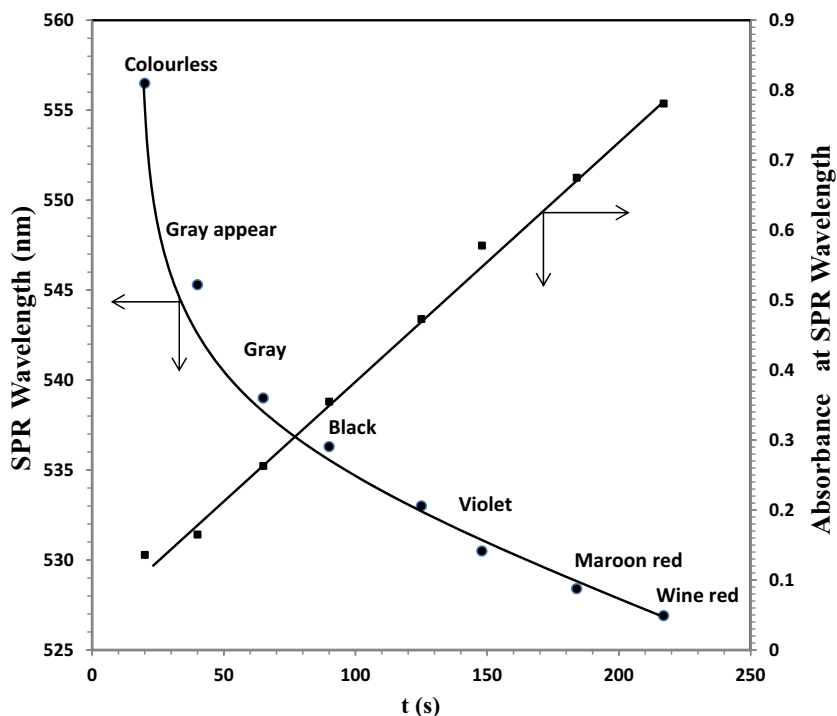
AuNP synthesis by the Turkevich method can be described as follows:

$$2\,[AuCl_4]^- + 3 \quad \text{(citric acid)} \longrightarrow 2\,Au^0 + 3 \quad \text{(dicarboxyacetone)} + 3\,H^+ + 8\,Cl^- \tag{1}$$
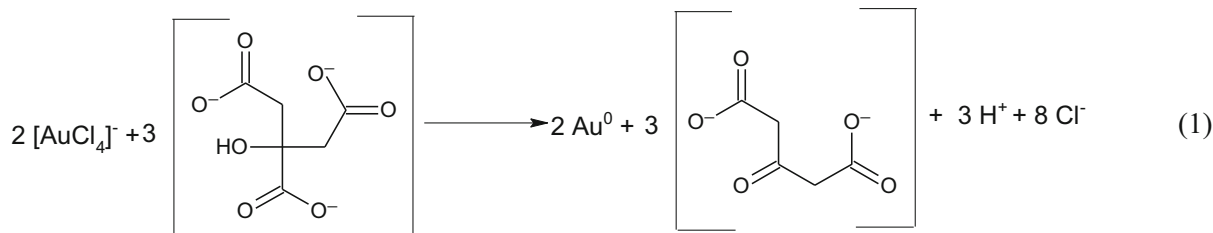
where 2 molecules of chloroauric acid is reduced by 3 molecules of trisodium citrate to produce 2 atoms of elemental gold and 3 molecules of dicarboxyacetone.

Kinetic study under baseline reaction conditions

Concentration of chloroauric acid in the samples was measured directly by monitoring UV spectroscopic absorbance at 212.5 nm and cross-checked by iodometric titration method [19, 26]. Colors and UV-Vis spectrophotometer data of samples collected during synthesis are shown in Fig. 1. SPR wavelengths and absorbance of samples collected at different time intervals are plotted in Fig. 2. During reaction, as color of the reaction medium changed from colorless to wine red, SPR peak decreased exponentially from 556.5 to 527.1 nm, indicating a blue shift during progress of the reaction [5]. Origin of SPR is attributed to collective oscillation of free conduction electrons [27] and SPR peak of the reaction medium is indicative of AuNP particle size, shape, and morphology [8, 13, 28, 29]. SPR peak and absorbance of gold sol are determined by refractive indices of the surrounding medium and multilayer coatings that are present on AuNP surfaces. Multiple scattering theory, which accounts for reduced mean free paths of conduction electrons on AuNPs, has been used for prediction of optical properties of gold sol [16]. SPR wavelength corresponding to maximum extinction shifts to longer wavelength as the size of AuNP is reduced [26]. Direction of wavelength shift depends on AuNP shape, size, and morphology—both blue and red shifts for gold sol have been reported by several investigators [12, 13].

The linear absorbance-time profile shown in Fig. 2 has been investigated by previous investigators [30] and is attributed to the complex formation mechanism of AuNP particles–homogeneous reduction of the precursor, disproportionation of the reactive intermediates, nucleation, and growth of AuNPs in the reaction medium.

Rate equation for consumption of chloroauric acid may be written as

$$\text{Rate} = -\frac{dC_A}{dt} = k_0\,C_A^m\,C_B^n \tag{2}$$

where C_A and C_B represent concentrations of chloroauric acid and trisodium citrate in the reaction medium. Reaction stoichiometry (Eq. 1) suggests complete reduction of the precursor at $M = 1.5$. However, published experimental data [22] suggest complete reduction of 3 mol of auric chloride by 1 mol of citrate ($M = 0.33$). Frens [10] reported complete conversion of auric chloride at $M = 0.43$. The discrepancy between the stoichiometric requirement and experimental data was ascribed to further degradation of dicarboxyacetone to form smaller molecules which reduce chloroauric acid to produce elemental gold [22]. In baseline experiments, $M = 1.33$ was maintained, and thus, citrate was assumed to be present in large excess in the reaction medium.

The reduction kinetics may be represented by a pseudo-mth order reaction given as follows:

$$\text{Rate} = -\frac{dC_A}{dt} = k\,C_A^m \tag{3}$$

A log-log plot of rate versus concentration of chloroauric acid data under baseline conditions yields values of k and m. From Fig. 3, values of rate constant $k = 8.79 \times 10^{-3}$ s^{-1} and $m = 1.067$ were obtained ($r = 0.946$). In our kinetic model, AuNP synthesis was considered as a pseudo-first-order reaction ($m = 1$) with respect to HAuCl$_4$ and repeated experiments at baseline reaction conditions confirm a first-order exponential decay (Eq. 4) of chloroauric acid concentration with time [19].

$$C_A = C_{A0}\,e^{-k\,t} \tag{4}$$

About 30 experiments were conducted at the baseline condition and from the slopes of ln (C/C_0) vs. time data rate constant values were calculated [$k = (7.93 \pm 0.67) \times 10^{-3}$ s^{-1}].
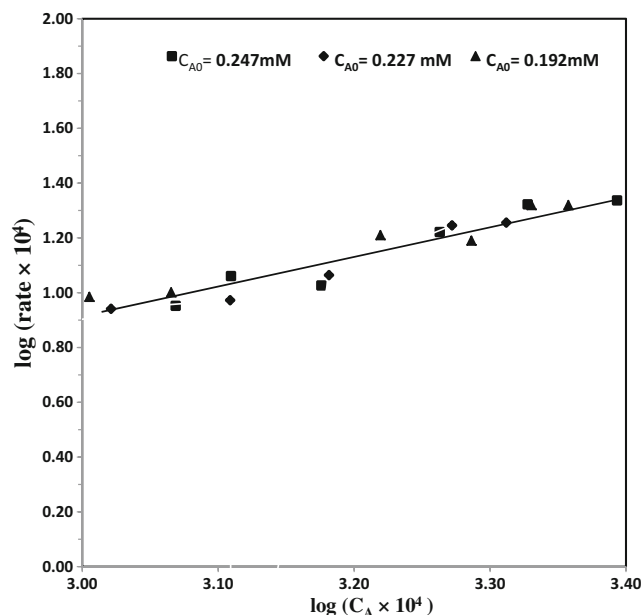
Fig. 3 Log-log plot of rate vs. concentration of chloroauric acid ($M = 1.33$, $T = 373$ K)

Pacławski et al. [15] reported experimental data on kinetics of AuNP formation using hydrazine as a reducing agent. They made several simplifying assumptions which reduced the Finke-Watzki model to a pseudo-first-order model, and the derived rate constant values varied between 1.6×10^{-3} and 6.5×10^{-3} s^{-1} which compares well with the values reported in this paper.

The entire process of formation of the AuNPs—reduction of precursor, formation of different ionic species, intermediate products and their network of complex reactions, physical processes involving transport of gold atoms and ions across the liquid–solid interface, and finally nucleation and aggregation of the gold atoms to form larger nanoparticles—is extremely complex. Description of such a complex process by a pseudo-first-order kinetic model is overly simplistic. However, in the absence of any experimental data and a suitable model on global kinetics to relate the complex network of physical and chemical processes, the pseudo-first-order kinetic model may be utilized for scaling-up and commercial-scale preparations of AuNPs.

A parity plot showing experimental data (dimensionless concentration vs. time) collected under baseline synthesis conditions and those predicted by Eq. 4 is shown in Fig. 4. It may be inferred from the plot that during the initial phase of the reduction process (<60–80 s), overall AuNP synthesis reaction may be adequately described by the pseudo-first-order kinetics (Eq. 4). Thereafter (>80 s), significant deviations were observed between experimental data and model predictions (Eq. 4)—the actual rate of reaction is significantly slower than that predicted by first-order global kinetics. This may be due to the fact that the initial rate of reaction is determined by

the intrinsic kinetics of the reaction, i.e., reduction of gold precursor. After 60–80 s, several complex reaction networks and transport processes compete with each other and the overall rate of reaction cannot be described by simple pseudo-first-order kinetics. At $t > 300$ s, when the AuNP particles attain maturity and significant sphericity, precursor concentration approaches a nonzero value, which changes with varying temperature and pH (Figs. 12 and 13, which will be discussed later). A detailed and more in-depth mechanistic study, combining the chemical reaction and the transport processes is necessary to accurately model, evaluate, and predict the competitive rates of the overall reaction, particle formation, and growth kinetics.

Particle formation under baseline reaction conditions

AuNP formation and optical behavior of reaction medium is a subject of intensive research and at times contradictory and inconclusive. There are a few in-depth reviews available on particle formation mechanisms [7, 15]. Nucleation–growth mechanism [23] suggests that AuNP formation in an aqueous medium proceeds in several stages—precursor is reduced to form a supersaturated solution leading to formation of asymmetric primary particles, which with time grow to form mature, spherical secondary particles. Formation of primary particles and their subsequent maturing to secondary nanoparticles is strongly influenced by process conditions of the reacting medium. DLS (Fig. 4; AuNP diameter vs. time) and AFM studies (Figs. 5, 6, and 7) of samples collected from reaction medium under baseline condition show that gold
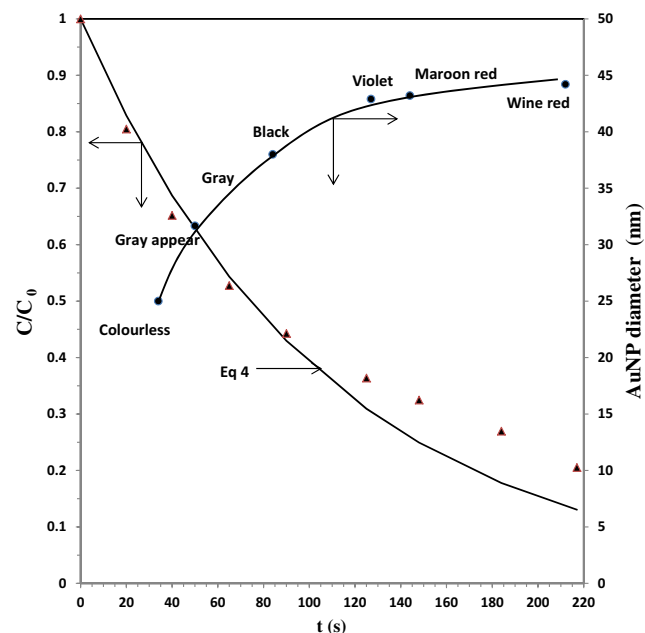

Fig. 4 Experimental data and model predictions (Eq. 4) on HAuCl$_4$ concentration and AuNP diameter vs. time under baseline reaction condition ($M = 1.33$, $T = 373$ K)
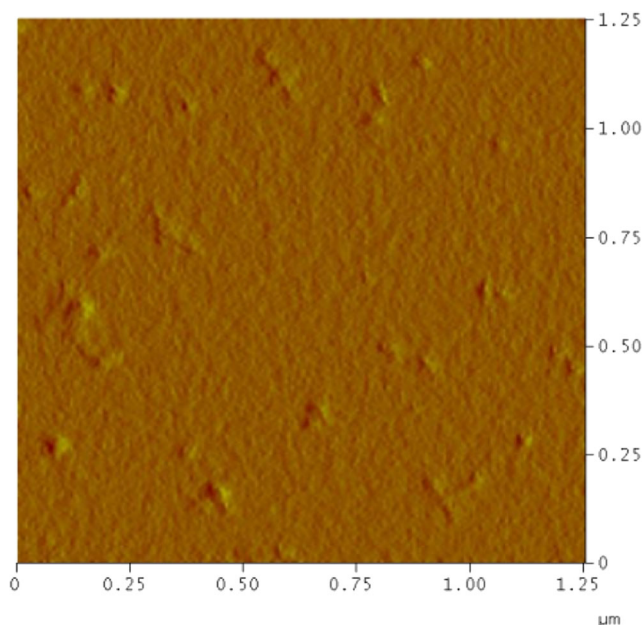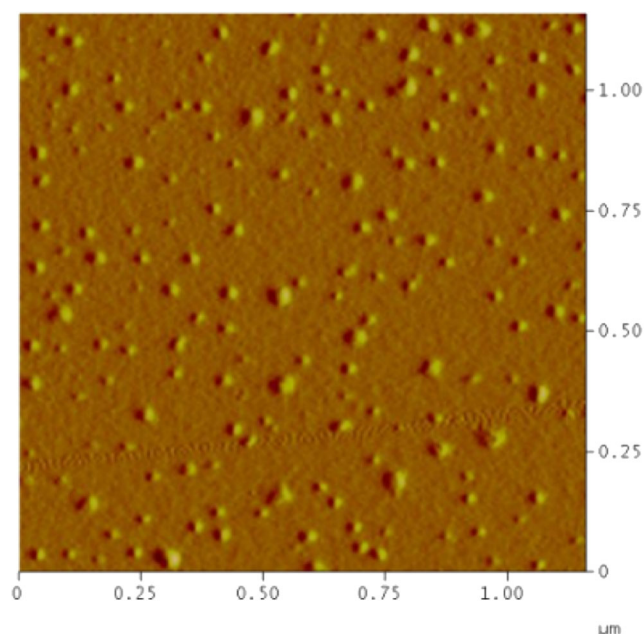
Fig. 5 AFM image of AuNPs 30 s after addition of trisodium citrate (gray solution)

particles gradually build up during the course of reaction. We could not detect any particle, either by DLS or AFM, within the first 20–30 s after addition of citrate to the boiling chloroauric acid solution. This lag period may be attributed to the time required for formation of the Au^{3+}-dicarboxyacetone complex [20], supersaturation of the reaction medium [14], and formation of an aggregate of critical size before a nucleus of the gold atom is formed [22]. Primary particles, which were found to be irregular, asymmetric, and nonspherical with about 24.5 ± 2.9 nm mean hydrodynamic
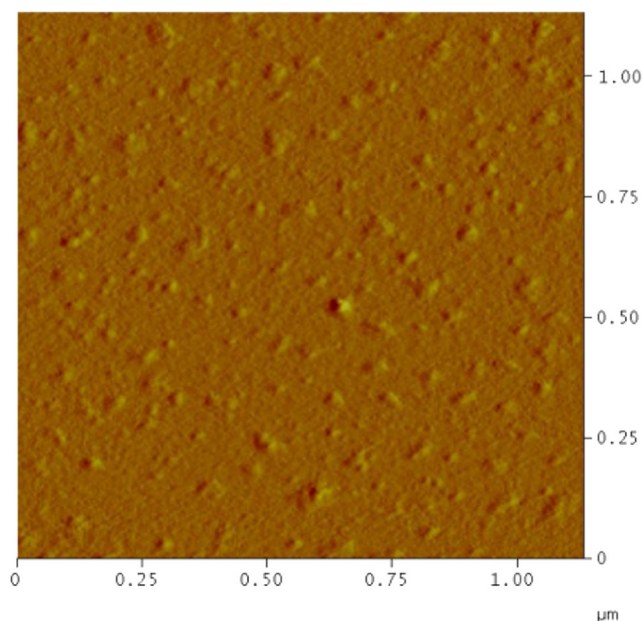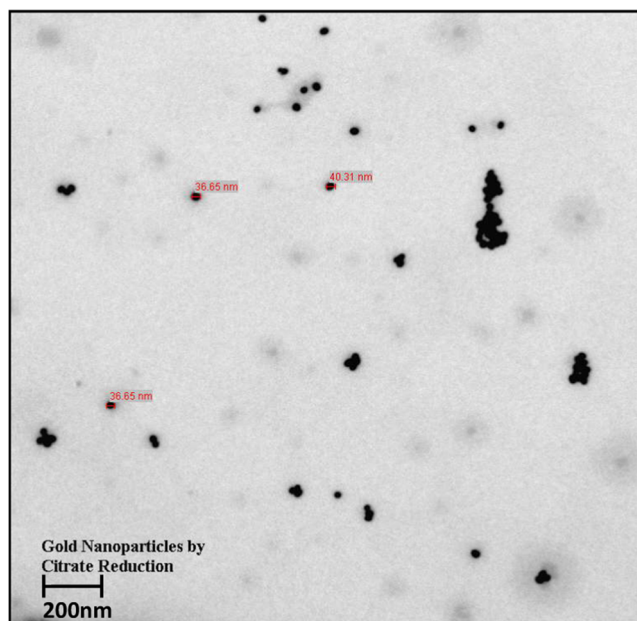

Fig. 6 AFM image of AuNPs 150 s after addition of trisodium citrate (violet solution)

diameter (Figs. 4 and 5), could be detected 25–30 s after addition of citrate to the reaction medium. These particles formed the nuclei for further growth to form secondary AuNPs. With time (30–150 s), these nonspherical nuclei became larger and more spherical in shape (Figs. 4 and 6). After about 200–250 s, the particles were found to be mature, symmetrical, and nearly spherical with about 44.31 ± 5.2-nm mean diameter (Figs. 4 and 7), although at times, significant polydispersity of AuNPs in the reaction medium was observed. Similar observations for AuNP shape and size were confirmed by TEM study (Fig. 8). Zabetakis [31] published experimental data and a detailed discussion on the effects of process conditions on hydrodynamic particle diameter and polydispersity of AuNP synthesized by the Turkevich-Frens method.

Our experimental data seem to support the nucleation–growth mechanism of AuNP formation [32] where each nucleus increases its size progressively until the final colloidal particle is formed. Zhang et al. [33] suggested that during AuNP synthesis, size of gold colloids increased with time due to Ostwald ripening process. Chow and Zukoski [23] reported formation of initially large AuNP particles of 100 nm or more in size and subsequent reduction of these clusters to smaller particles through a stabilization mechanism. Kimling et al. [13] proposed a multistep mechanism of particle formation—particle appearance, collapse to form larger particles, and growth of particles by the residual amount of reduced gold in solution. Kumar et al. [22] developed a population balance model to predict particle size distribution. They suggested that unlike the usual balance between nucleation and growth that determines particle size, it is the balance
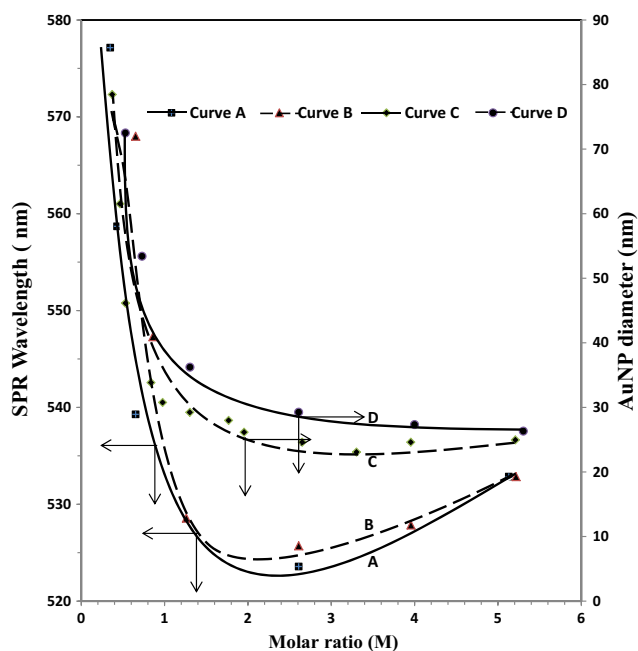

Fig. 7 AFM image of AuNPs 250 s after addition of trisodium citrate (wine red solution)

Fig. 8 TEM image of AuNPs 250 s after addition of trisodium citrate (wine red solution)

Fig. 9 Variation of SPR wavelength and AuNP diameter with initial molar ratio of the reactants (*M*): *curves A and C*—HAuCl₄ concentration = 0.0318–1.016 mM and citrate concentration = 34 mM; *curves B and D*—HAuCl₄ concentration = 0.254 mM and citrate concentration = 8.5–136.2 mM

between the rate of nucleation and degradation of dicarboxyacetone that determined particle size in the Turkevich process.

Effect of initial molar ratio of reactants on mean particle diameter

Frens [10] first pointed out that citrate concentration in the reaction medium has a profound influence on size and shape of the AuNPs. To investigate the effects of changing initial concentrations of chloroauric acid and trisodium citrate on reaction kinetics, experiments were performed at different initial molar ratios of reactants (M = 0.33 to 5.35; Fig. 9). Curves A and C represent experiments where initial concentration of chloroauric acid was increased from 0.0318 to 1.016 mM in several stages keeping concentration of citrate (34.3 mM) constant. Curves B and D represent experiments where concentration of citrate was decreased from 136 to 8.5 mM in several stages keeping concentration of HAuCl₄ constant (0.254 mM). Appropriate volumes of these reactants were mixed to maintain the desired molar ratio. These curves do not represent best-fit lines—they were drawn only for guiding the viewers. Final solutions obtained after 300-s reaction were analyzed using spectroscopy, DLS, and AFM. Plots of SPR wavelength (curves A and B) and mean particle diameter (curves C and D) vs. molar ratio are shown in Fig. 9. As the molar ratio was increased from 0.35 to 2.5, a steep drop in both SPR wavelength and AuNP diameter was observed. At molar ratio higher than 2.5, although the SPR wavelength increased, AuNP diameter remained nearly constant. Sivaraman et al. [11] reported similar results for AuNP

synthesis with tannic acid where at an optimum tannic acid to chloroauric acid molar ratio of 3, formation of 20 nm AuNP particles was observed. At higher molar ratio of the reactants, significant polydispersity of the aqueous medium was observed, which might have contributed to the observed changes in SPR wavelength. Similar observations were reported by other investigators [9, 22, 23, 34].

Rate of formation of gold nuclei is strongly dependent upon formation of Au⁺³-dicarboxyacetone complex which is favored by higher initial concentration of trisodium citrate. Thus, a higher molar ratio (M) results in a steep increase in the number of Au⁰ nuclei formed which in turn results in a sharp decrease in the observed particle diameter [22]. Curves A and B remain in close proximity, almost overlapping on each other, suggesting that SPR wavelength of the final colloidal solution, which is indicative of shape, size, and aspect ratio of the AuNPs formed, depends only on initial molar ratio of the reactants and is independent of the initial molar concentrations of either chloroauric acid or trisodium citrate. Similar conclusions can be drawn for the final particle diameters of the AuNP formed (curves C and D). In AuNP synthesis, molar ratio of reactants is an important process parameter which decides the rate of reaction, particle diameter, shape, size, and morphology of the nanoparticles. Kimling et al. [13] made an almost identical observation concluding that in the Turkevich method, the final size of the AuNP particles is decided by the

gold-to-reductant ratio and is independent of the absolute concentrations of the reactants. The SPR wavelength and particle diameter observed at baseline molar ratio ($M = 1.33$) were 527.5 ± 2.3 and 32.5 ± 1.6 nm, respectively (Fig. 9), which are the preferred parameters for AuNPs used in immunoassay and biomarker applications.

Investigations by other researchers on mean particle diameter against molar ratio support our experimental findings and conclusions [5, 7]. A summary plot of experimental data available in published literature [10, 22, 23, 34] and our experimental findings on mean particle diameters at different molar ratios is shown in Fig. 10. Our experimental data appear to follow almost identical trend reported by previous investigators. As molar ratio of citrate to chloroauric acid (M) in the reacting medium was increased, mean particle diameter of the final colloidal gold particles decreased dramatically till the molar ratio reached in the range 2.50–2.70. AuNP diameter at $M = 0.37$ was almost three times larger than the AuNP diameter at $M = 2.0$. Kumar [22] reported that AuNP size decreased by as much as a factor of 7 when the molar ratio was increased from 0.4 to 2.0. In our experiments, when the molar ratio was increased beyond 2.5, mean particle diameter of AuNPs did not change appreciably and remained nearly constant at 23.97 ± 1.35 nm. At higher molar ratio ($M > 1.5$), Kumar et al. [22] predicted that auric chloride becomes the limiting reactant, rate of nucleation becomes independent of the initial concentration of chloroauric acid, and particle size becomes independent of the initial molar ratio (M). For several biomedical applications, 20–40 nm is the desired AuNP size which may be achieved by choosing an appropriate reactant molar ratio [13, 35].
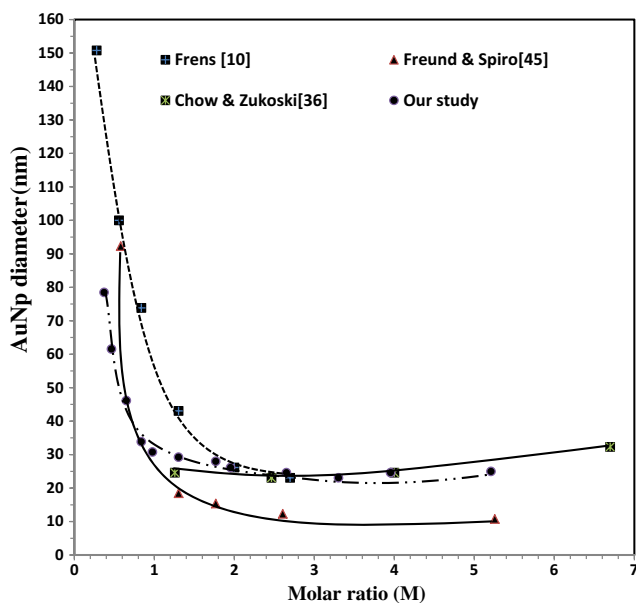
Effect of initial molar ratio of reactants on rate constant

To investigate the effect of molar ratio of reactants on reaction kinetics, time–concentration profiles of chloroauric acid at different initial molar ratios of reactants ($M = 0.33$ to 5.35), as described earlier, were utilized to calculate values of pseudo-first-order rate constants (k) (correlation coefficient of $\ln (C/C_0)$ vs. time data varied between 0.854 and 0.956). In Fig. 11, curve A shows a plot of k values vs. molar ratio for change of initial chloroauric acid concentration (0.0318–1.016 mM) and a fixed concentration of trisodium citrate (34.3 mM). Curve B shows a plot of k values vs. molar ratio for change of concentration of citrate (8.5–136.2 mM) and a fixed concentration of HAuCl$_4$ (0.254 mM). It may be observed that change in molar ratio has a significant impact on reaction kinetics. The maximum value of rate constant of the reduction reaction was observed near baseline molar ratio $M = 0.75$–1.35. If molar ratio is increased or decreased beyond this optimum range by changing initial concentration of either chloroauric acid or that of trisodium citrate, values of rate constant (k) always decreased from the maximum value (6.8×10^{-3}–7.0×10^{-3} s^{-1}), indicating that the reaction is fastest near
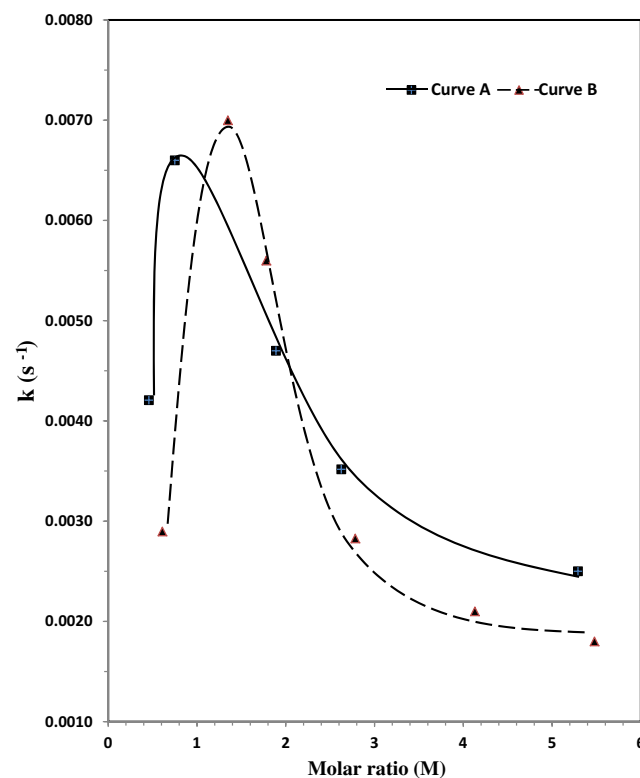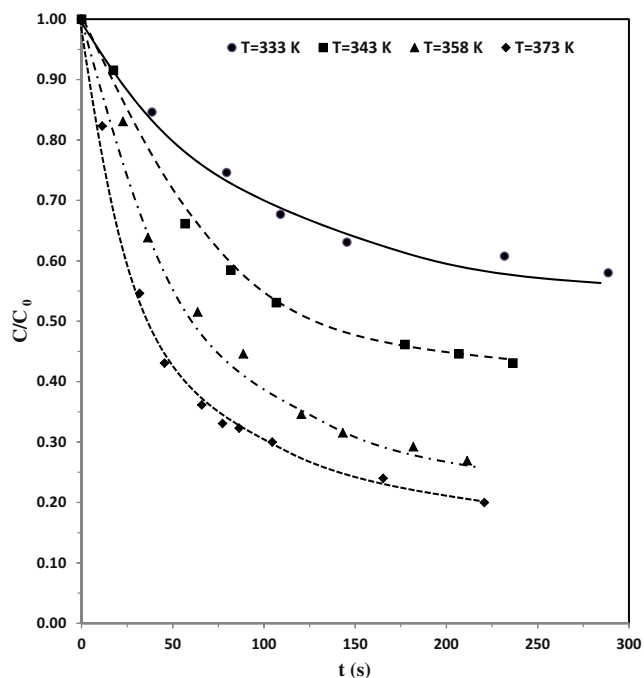
Fig. 11 Variation of pseudo-first-order rate constant with initial molar ratio of the reactants (M): *curve A*—HAuCl$_4$ concentration = 0.0318–1.016 mM and citrate concentration = 34.3 mM; *curve B*—HAuCl$_4$ concentration = 0.254 mM and citrate concentration = 8.5–136.2 mM

Fig. 10 AuNP diameter vs. molar ratio of the reactants [22]

the baseline molar ratio. Any value of M, lower or higher than the optimum value, will slow down the reaction rate. This optimal range of M may be utilized for large-scale synthesis of AuNPs for the fastest reaction kinetics, desired particle diameter, shape, size, and morphology.

Effect of temperature of the reaction medium

As expected for a pseudo-homogeneous reaction, temperature of the reaction medium has a significant effect on formation kinetics of AuNPs. Experiments were conducted at baseline molar ratio of 1.33 ± 0.053 while temperature of the reaction medium was varied between 333 and 373 K by carrying out AuNP synthesis in a temperature-controlled bath (± 1 K). In all of these experiments, exponential decrease in concentration of chloroauric acid with time was observed (Fig. 12). From an Arrhenius plot of rate constant data, preexponential factor ($A = 8.013 \pm 0.896$ mM s^{-1}) and activation energy ($E = 21.69 \pm 2.3$ kJ/mol) were calculated ($r = 0.832$). The estimated value of activation energy for the AuNP synthesis reaction is typical of a pseudo-homogenous reaction and lends support to the hypothesis that reduction of chloroauric acid occurs in aqueous phase and is followed by diffusion-controlled nucleation and aggregation of reduced metal ions to form larger nanoparticles. At lower temperatures (333 and 343 K), the shape of the AuNPs was more asymmetric and nonspherical than that of the particles formed at higher temperatures (358 and 373 K). AuNPs prepared at higher temperatures (358 and 373 K) were more stable than those prepared

at lower temperatures (333 and 343 K). Global kinetics of the AuNP synthesis reaction can be represented by Eq. 5.

$$\text{Rate} = -\frac{dC_A}{dt} = (8.013 \pm 0.896)\, e^{-\left(\frac{21.69 \times 10^3}{RT}\right)} C_A \qquad (5)$$

Change of pH of the reaction medium

In baseline experiments, pH of 0.254 mM chloroauric acid solution was 3.18 while that of 0.34 mM trisodium citrate was 8.44. During reaction, pH of the reaction medium changed continuously and pH of the final reaction mixture was observed to be equal to 3.6 ± 0.23. To investigate the effect of pH on reduction kinetics, experiments were conducted at baseline molar ratio while pH of reaction medium was adjusted between 3.6 and 6.5 by adding 75–500 μl of 0.1 M NaOH. At pH lower than 3.6, an additional peak at 314 nm appeared in the UV-Vis spectrum [30] and estimation of chloroauric acid concentration became difficult; results of these experiments are not reported here. We could not carry out experiments at pH higher than 6.5 because even after 300 s, no substantial change in color, SPR wavelength, or concentration of chloroauric acid in the reaction medium could be detected.

Normalized concentration vs. time profiles of chloroauric acid at different pH of the reaction medium are shown in Fig. 13. In the pH range 3.6–5.2, exponential decay of time–

Fig. 12 Time–concentration profile of HAuCl$_4$at different reaction temperatures; $M = 1.33$
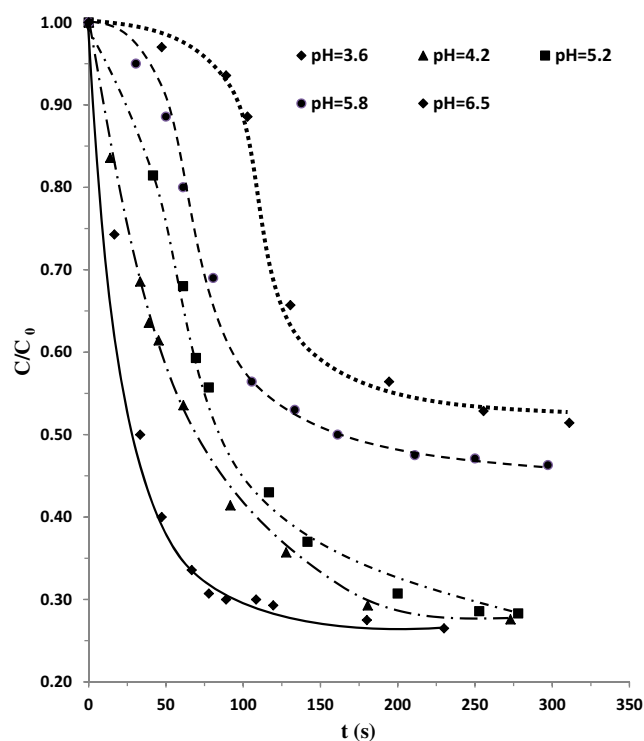
Fig. 13 Time–concentration profile of HAuCl$_4$ for different pH of the reaction medium; M = 1.33

concentration profile, indicative of pseudo-first-order kinetics, was observed. At pH higher than 5.2, the time–concentration profile showed distinct deviation, suggesting an onset of shift in the reduction–particle formation mechanism [14]. At near neutral pH (6.5), after an initial lag phase (no color change or significant concentration change of chloroauric acid until about 80–100 s), a steep fall in concentration of chloroauric acid was observed. This could be due to slow diffusion-controlled growth followed by a rapid nucleation of gold particles [14]. Molecular forces between citrate protection groups and gold surfaces [22] and zeta potential of AuNPs are strongly pH dependent [2, 13]. At lower pH (3.6–5.2), the well-defined kinetics could be attributed to the presence of the highly reactive $AuCl_3(OH)]^-$ as the sole oxidant [20]. At pH > 6.5, very reactive $[AuCl_3(OH)]^-$ is converted to less reactive $[AuCl_2(OH)_2]^-$ and $[AuCl(OH)_3]^-$, following substantially different mechanistic pathways of AuNP formation [23]. Henglein and Giersig [32] reported a significant influence of pH on growth of silver nanoparticles.

pH of the reaction medium is an important process parameter that influences gold sol stability. Electrostatic repulsions of negatively charged citrate ions keep AuNPs well-dispersed in a gold sol. At pH <4, the color of gold sol changed from wine red to purple after 15 days indicating an onset of aggregation process. At low pH, citrate ions are fully protonated and contribute to reduced stability of the gold sol [34, 36]. Wine red color of AuNP sol synthesized in the pH range 3.6–5.2 persisted for more than a month indicating higher stability. These observations were supported by detailed AFM images.

Conclusion

Time-variant precursor concentrations in the reaction medium were measured directly by recording absorbance of the reaction medium at 212.5 nm and cross-checked by iodometric estimation method. AuNP synthesis could be suitably modeled by a pseudo-first-order kinetics, and rate constant values at a fixed baseline condition were reported. The model is valid over a narrow and limited range of practical applicability—more specifically during the initial period of reaction (<80 s). The reaction proceeds further deviation between model predictions and experimental data grow wider, probably due to the fact that several complex reaction networks and mass transport processes compete with each other and the overall rate of reaction can no longer be described by a simple pseudo-first-order kinetics. During reaction, SPR peak of the reaction medium decreased from 556.5 to 527.1 nm in about 250 s. Twenty-five to 30 s after addition of the citrate to an aqueous solution of the precursor, irregular shape, nonspherical primary particles of 24.5 ± 2.9 were detected in the reaction medium. With time, these primary particles grew bigger,

attained maturity, and became more spherical. After about 300 s, near-perfect spherical AuNPs were formed, although depending upon the process operating conditions, significant polydispersity of the reaction medium was observed. Mole ratio of reactants in baseline experiment was maintained at 1.33 ± 0.053 where the fastest reaction rate and AuNP spherical symmetry were observed. The final particle diameter of AuNPs could be controlled by changing reactant molar ratios and process operating conditions. Any increase or decrease beyond the optimal molar ratio ($M = 0.75$–1.35) led to a slower reaction rate, larger particle diameter, and higher peak absorption wavelength (blue shift) resulting in formation of AuNPs which were unsuitable for biological applications. Influences of process parameters—temperature, pH, and molar ratio of reactants on kinetic rate parameters and morphology of formation of AuNP—were discussed. Exponential decrease of precursor concentration was observed at or below pH = 5.2 of the reaction medium. At pH >5.2, a distinct deviation of the mechanistic pathway of the AuNP formation was observed. Optimal conditions for producing desired particle diameter, morphology, and reaction kinetics were identified and reported.

References

1. Link S, El-Sayed MA (1999) Size and temperature dependence of the plasmon absorption of colloidal gold nanoparticles. J Phys Chem B 103:4212
2. Haiss W, Thanh NT, Aveyard J, Fernig DG (2007) Determination of size and concentration of gold nanoparticles from Uv−Vis spectra. Anal Chem 79:4215
3. Sinha AK, Seelan S, Tsubota S, Haruta M (2004) Catalysis by gold nanoparticles: epoxidation of propene. Top Catal 29:95
4. Mertens P, Corthals S, Ye X, Poelman H, Jacobs P, Sels B, Vankelecom I, De Vos D (2009) Selective alcohol oxidation to aldehydes and ketones over base-promoted gold–palladium clusters as recyclable quasihomogeneous and heterogeneous metal catalysts. J Mol Catal A Chem 313:14
5. Lin CAJ, Yang TY, Lee CH, Huang SH, Sperling RA, Zanella M, Li JK, Shen JL, Wang HH, Yeh HI (2009) Synthesis, characterization, and bioconjugation of fluorescent gold nanoclusters toward biological labeling applications. ACS Nano 3:395
6. Basu M, Seggerson S, Henshaw J, Jiang J, Cordona RA, Lefave C, Boyle PJ, Miller A, Pugia M, Basu S (2004) Nano-biosensor development for bacterial detection during human kidney infection: use of glycoconjugate-specific antibody-bound gold nanowire arrays. Glycoconj J 21:487
7. Daniel MC, Astruc D (2004) Gold nanoparticles: assembly, supramolecular chemistry, quantum-size-related properties, and applications toward biology, catalysis, and nanotechnology. Chem Rev 104:293
8. Baptista P, Pereira E, Eaton P, Doria G, Miranda A, Gomes I, Quaresma P, Franco R (2008) Gold nanoparticles for the development of clinical diagnosis methods. Anal Bioanal Chem 391:943
9. Turkevich J, Stevenson PC, Hillier J (1951) A study of nucleation and growth processes in the synthesis of colloidal gold. Discus Faraday Soc 11:55

10. Frens G (1973) Controlled nucleation for the regulation of the particle size in monodisperse gold suspensions. Nature 241:20

11. Sivaraman SK, Kumar S, Santhanam V (2010) Room-temperature synthesis of gold nanoparticles-size-control by slow addition. Gold Bull 43:275

12. Sivaraman SK, Kumar S, Santhanam V (2011) Monodisperse sub-10 nm gold nanoparticles by reversing the order of addition in Turkevich method—the role of chloroauric acid. J Colloid Interface Sci 361:543

13. Kimling J, Maier M, Okenve B, Kotaidis V, Ballot H, Plech A (2006) Turkevich method for gold nanoparticle synthesis revisited. J Phys Chem B 110:15700

14. Ji X, Song X, Li J, Bai Y, Yang W, Peng X (2007) Size control of gold nanocrystals in citrate reduction: the third role of citrate. J Am Chem Soc 129:13939

15. Paclawski K, Streszewski B, Jaworski W, Luty-Blocho M, Fitzner K (2012) Gold nanoparticles formation via gold(III) chloride complex ions reduction with glucose in the batch and in the flow microreactor systems. Colloids Surf A Physicochem Eng Asp 413:208

16. Bastus NG, Comenge J, Puntes V (2011) Kinetically controlled seeded growth synthesis of citrate-stabilized gold nanoparticles of up to 200 nm: size focussing versus Ostwald ripening. Langmuir 27:11098

17. Watzky MA, Finke RG (1997) Transition metal nanocluster formation kinetic and mechanistic studies: a new mechanism when hydrogen is the reductant: slow, continuous nucleation and fast autocatalytic surface growth. J Am Chem Soc 119:10382

18. Patakfalvi R, Papp S, Dekany I (2007) The kinetics of homogeneous nucleation of silver nanoparticles stabilized by polymer. J Nanopart Res 9:353

19. Chakraborty A, Chakraborty S, Chaudhuri B, Bhanacharjee S (2012) Spectroscopic estimation of chloroauric acid during synthesis of gold nanoparticles by citrate reduction method. Adv Sci Eng Med 4:128

20. Ojea-Jimenez I, Bastus NG, Puntes V (2011) Small gold nanoparticles synthesized with sodium citrate and heavy water: insights into the reaction mechanism. J Phys Chem C 115:15752

21. Polte JR, Aimer TT, Delissen F, Sokolov S, Emmerling F, Thunemann AF, Kraehnert R (2010) Mechanism of gold nanoparticle formation in the classical citrate synthesis method derived from coupled in-situ XANES and SAXS evaluation. J Am Chem Soc 132:1296

22. Kumar S, Gandhi K, Kumar R (2007) Modeling of formation of gold nanoparticles by citrate method. Ind Eng Chem Res 46:3128

23. Chow M, Zukoski C (1994) Gold sol formation mechanism: role of colloidal stability. J Colloid Interface Sci 165:97

24. Okitsu K, Ashokkumar M, Grieser F (2005) Sonochemical synthesis of gold nanoparticles: effects of ultrasound frequency. Phys Chem B 109:20673

25. Peck JA, Tait CD, Swanson BI, Brown GE (1991) Speciation of aqueous gold(III) chlorides from ultraviolet/visible absorption and Raman/resonance Raman spectroscopies. Geochim Cosmochim Acta 55:671

26. Chow A, Beamish F (1963) Studies of titrimetric and spectrophotometric methods for the determination of gold. Talanta 10:883

27. Itoh H, Naka K, Chujo Y (2004) Synthesis of gold nanoparticles modified with ionic liquid based on the imidazolium cation. J Am Chem Soc 126:3026

28. Zhou J, Ralston J, Sedev R, Beattie DA (2009) Functionalized gold nanoparticles: synthesis, structure and colloid stability. J Colloid Interface Sci 331:251

29. Suman T, Rajasree SR, Ramkumar R, Rajthilak C, Perumal P (2014) The Green synthesis of gold nanoparticles using an aqueous root extract of Morinda citrifolia. Spectrochim Acta, Part A 118:11

30. Turkevich J (1985) Colloidal gold. Part I: historical and preparative aspects, morphology and structure. Gold Bull 18:86

31. Zabetakis K, Ghann WE, Kumar S, Daniel MC (2012) Effect of high gold salt concentrations on the size and polydispersity of gold nanoparticles prepared by an extended Turkevich-Frens method. Gold Bull 45:203

32. Pong BK, Elim HI, Chong JX, Ji W, Trout BL, Lee JY (2007) New insights on the nanoparticle growth mechanism in the citrate reduction of gold(III) salt: formation of the Au nanowire intermediate and its nonlinear optical properties. J Phys Chem C 111:6281

33. Zhang G, Jasinski JB, Howell JL, Patel D, Stephens DP, Gobin AM (2012) Tunability and stability of gold nanoparticles obtained from chloroauric acid and sodium thiosulfate reaction. Nanoscale Res Lett 7:1

34. Freund PL, Spiro M (1985) Colloidal catalysis: the effect of sol size and concentration. J Phys Chem 89:1074

35. Liu Z, Zu Y, Guo S (2009) Synthesis of micron-scale gold nanochains by a modified citrate reduction method. Appl Surf Sci 255:5827

36. Wager K, Chui T, Adem S (2014) Effect of pH on the stability of gold nanoparticles and their application for melamine detection in infant formula. IOSR-JAC 7:8